Research Article

Ekaterina E. Maslova, Mikhail V. Rybin, Andrey A. Bogdanov* and Zarina F. Sadrieva

Bound states in the continuum in periodic structures with structural disorder

https://doi.org/10.1515/nanoph-2021-0475
Received August 23, 2021; accepted October 27, 2021;
published online November 11, 2021

Abstract: We study the effect of structural disorder on the transition from the bound states in the continuum (BICs) to quasi-BICs by the example of the periodic photonic structure composed of two layers of parallel dielectric rods. We uncover the specificity in the robustness of the symmetry-protected and accidental BICs against various types of structural disorder. We analyze how the spatial mode localization induced by the structural disorder results in an effective reduction of the system length and limits the Q factor of quasi-BICs. Our results are essential for the practical implementation of BICs especially in natural and self-assembled photonic structures, where the structural disorder plays a crucial role.

Keywords: bound states in the continuum; metasurface; spatial localization; structural disorder.

1 Introduction

Bound states in the continuum (BICs) are the specific solutions of the wave equation which are spatially localized despite the fact that their frequencies lay in the radiation continuum. Initially, BICs were proposed in quantum mechanics by von Neumann and Wigner [1]. In the last two decades, BICs have been observed in many photonic structures such as photonic crystals, metasurfaces [2–4], chains of coupled resonators [5–8], waveguides [9–13], and even single subwavelength resonators supporting quasi-BIC in a form of supercavity modes [14–16]. A divergent radiative quality (Q) factor, strong spatial localization, and drastic enhancement of the incident field make BICs very prospective for many applications including lasers [17–25], optical filters [26–28], biological and chemical sensors [29–33], and nonlinear photonics [34–43].

A genuine BIC with an infinitely large radiative Q factor is a mathematical idealization. In real samples, the radiative Q factor becomes finite due to roughness, diffraction on the edges and into the substrate, and other imperfections inevitably appearing during the fabrication. Thus, in practice, a genuine BIC turns into a *quasi-BIC* (q-BIC) manifesting itself in the scattering spectra as a high-Q resonance [44–47]. The material absorption also results in a decrease in the total Q factor of q-BIC and makes it hardly recognizable in the experimental scattering spectra. The identification of the dominant loss mechanism is the crucial point allowing enhancing the performance of the photonic devices based on BICs.

Most of the systems supporting q-BIC are periodic (metasurfaces, grating, chains etc.). The *structural disorder* in such systems drastically affects their optical properties resulting in nontrivial Fano resonance evolution, light localization, and coherent back-scattering etc. [48–52]. The disorder effects are most essential in self-assembled and natural photonic structures [53–55]. Despite the important role of the structural disorder in periodic photonic structures, it is weakly studied in application to BICs and their transition to q-BICs. In particular, the coupled-wave theory (CWT) framework was developed to study the Q factor of symmetry-protected BIC in dielectric gratings with randomly perturbed filling factor and the element position [56]. The radiation losses of symmetry-protected BICs were shown to decrease quadratically with the fluctuation amplitude. It was shown in Ref. [57] that disorder can results in the formation of BIC band in multichain and multilayer systems. The robustness of symmetry-protected BICs was partly analyzed in Ref. [58] in the framework of the Fano–Anderson model applied to the system of parallel coupled waveguide.

Here we provide a rigorous analysis of the Q factor of both symmetry-protected and accidental BICs in a two-layered periodic array of infinitely long dielectric rods

***Corresponding author: Andrey A. Bogdanov**, School of Physics and Engineering, ITMO University, 197101, St. Petersburg, Russia; and Ioffe Institute, 194021, St. Petersburg, Russia,
E-mail: a.bogdanov@metalab.ifmo.ru. https://orcid.org/0000-0002-8215-0445
Ekaterina E. Maslova and Zarina F. Sadrieva, School of Physics and Engineering, ITMO University, 197101, St. Petersburg, Russia,
E-mail: z.sadrieva@metalab.ifmo.ru (Z. F. Sadrieva)
Mikhail V. Rybin, School of Physics and Engineering, ITMO University, 197101, St. Petersburg, Russia; and Ioffe Institute, 194021, St. Petersburg, Russia

accounting for the structural disorder in the position of the rods keeping them parallel, i.e. preserving the translation symmetry. In contrast to the Ref. [56], we uncover two concurrent radiation loss mechanisms due to a finite number of periods and scattering due to the structural disorder. We find the disorder amplitude up to which the vertical and horizontal fluctuations in the rod position contribute to the radiation losses independently. We demonstrate that accidental BIC is more resistant to the fluctuation of the position along the direction of periodicity rather than to the perturbation of distance between two layers of rods. Contrary, the symmetry-protected BIC shows greater sensitivity to the fluctuation of the distance between the layers. Also, we reveal the disorder-induced spatial localization of the q-BICs and prove that it limits the Q factor of q-BICs if the array of rods is longer than the localization length.

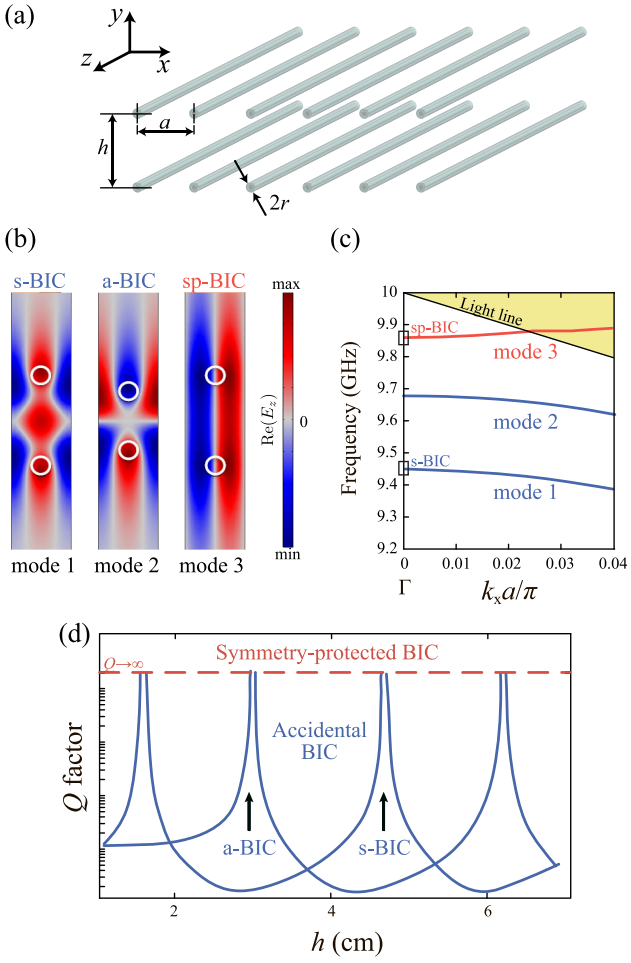

Figure 1: Bound states in the continuum in two-layered structure of infinite dielectric rods. (a) Schematic view of the photonic structure. (b) Electric field E_z distribution of accidental (mode 1, mode 2) and symmetry-protected (mode 3) BICs in the Γ-point. The mode profiles are plotted for different distances between layers h ($h = 4.7$ cm for modes 1 and 3; $h = 3$ cm for mode 2). (c) The band diagram of TE-polarized modes. (d) Q factor versus distance between layers h.

2 Results and discussions

2.1 Infinite array without structural disorder

We start the analysis from the consideration of the infinite periodic structure without structural disorder shown in Figure 1(a). It consists of two identical periodic arrays of infinitely long dielectric rods. The radius of the rods $r = 0.5$ cm and the period $a = 3$ cm. Thus, the unit cell of the structure contains two rods spaced apart by distant h. For further analysis we will use permittivity of the rods $\varepsilon = 2.1$ that corresponds to low-loss polymers, for example, Teflon in the frequency range 0.1–10 GHz [59, 60]. The advantage of such low-refractive-index materials is that the electromagnetic field is mostly localized outside the rods, i.e. in air, where the losses are negligible. Thus, the material absorption is substantially suppressed substantially and we will not account for it in the further analysis. The considered two-layer system is convenient as it provides a simple way to precisely tune the accidental and symmetry-protected BICs [61–67].

According to the Bloch theorem, the electric field of eigenmodes can be written as $\mathbf{E}(x,y,z) = \mathbf{U}_{s,k_x}(x,y)\,e^{ik_x x + ik_z z}$. Here, k_z is the wavenumber corresponding to the direction of the translation symmetry, k_x is the Bloch wavenumber, s is the index of the band and we will omit for simplicity, $\mathbf{U}_{s,k_x}(x,y)$ is the periodic function of x. The BICs in such system appear only if either $k_z = 0$ or $k_x = 0$. Further, we will limit our analysis to the case of TE-polarized modes [$\mathbf{E} = (0,0,E_z)$] with $k_z = 0$. For TE modes with $k_z = 0$, we can write $E_z(x,y) = U_{k_x}(x,y)e^{ik_x x}$. The periodic Bloch amplitude can be expanded into the Fourier series as follows:

$$U_{k_x}(x,y) = \sum_n C_{n,k_x}(y)e^{i\frac{2\pi n}{a}x}, \tag{1}$$

where n is the index of the diffraction channel. At the frequencies above the light line ($\omega/c > |k_x|$), the mode leaks from the structure to the radiation continuum via the open diffraction channels. BIC appears when the leakage into all open diffraction channels is forbidden, i.e. the complex Fourier coefficients $C_{n,k_x}(y)$ – the amplitudes of the outgoing waves – are zero. In the subwavelength regime $\lambda < a$, only the zeroth diffraction channel is open. Thus, the amplitude of the outgoing leaky wave is defined by the zeroth Fourier coefficient $C_{0,k_x}(y)$. By the

definition, it is equal to the field averaged over the period, i.e. $C_{0,k_x}(y) = \langle U_{0,k_x}(x,y)\rangle_x$. For the structures having the time-reversal and π-rotational symmetries, denoted as TC_2^y, the coefficient $C_{0,k_x}(y)$ becomes pure real for BICs [68–70]. At the Γ-point (the center of the Brillouin zone), $U_{k_x}(x,y)$ is either odd or even function of x since the photonic structure is C_2^y-invariant [71, 72]. Obviously, for an odd function $U_{k_x}(x,y)$ the zero-order Fourier coefficient vanishes. In this case, the *symmetry-protected* BIC occurs – the coupling to the radiation continuum disappears due to the point-symmetry of the structure. In the case of the even mode, the spatial average $\langle U_{0,k_x}(x,y)\rangle_x$ may vanish not only due to the symmetry reasons but at specific values of the structure parameters such as period, the radius of rods, permittivity, interlayer distance resulting in the appearance of *accidental* BIC also called *tunable* BIC.

Figure 1(b) and (c) show the spectra of TE-modes and the electric field distribution for possible BICs appeared in the Γ-point. Mode 3 is odd with respect to C_2^y transformation and, thus, it has a symmetry-protected BIC labeled as sp-BIC. Modes 1 and 2 are even with respect to C_2^y transformation and, thus, they can have only accidental BICs. The dependence of the Q factor for all three modes in the Γ-point versus the distance between the layers h is shown in Figure 1(d). One can see from this figure that the BICs in the Γ-point of modes 1 and 2 appear only at the specific distances between the layers, while the Q factor of the sp-BIC is insensitive to h. The spectral position of the Γ-point for all three modes versus h is shown in Figure 6 in Appendix A. Modes 1 and 2 have different symmetries with respect to the $y \to -y$ transformation. Mode 1 is even (symmetric) and mode 2 is odd (anti-symmetric). Thus, we denote the corresponding BICs as s-BIC and a-BIC. These BICs can be considered as Fabry–Perot resonances formed due to the total reflection from the array of the rods [5, 73, 74].

2.2 Structural disorder and *Q* factor

In this section, we consider the structure of finite size, consisting of N periods, accounting for the structural disorder. In this case, the total Q factor is contributed by two parts

$$\frac{1}{Q_{\text{tot}}} = \frac{1}{Q_{\text{ord}}} + \frac{1}{Q_{\text{dis}}} \tag{2}$$

as we neglect absorption and the effect of surface roughness. Here, Q_{dis} is responsible for the radiation due to the structural disorder; Q_{ord} is responsible for the radiation due to the finite size of the structure and it is a function of N. Since the finite structure is not true periodic, the diffraction directions are smeared out resulting in additional diffraction losses. Therefore, a genuine BIC transforms into a resonant state (quasi-BIC) with finite Q factor [7, 75]. Recently, the Q factor of a symmetry-protected quasi-BIC was shown to grow as $\sim N^2$, see Ref. [76], while the Q factor of an accidental quasi-BIC emerging at the center of the Brillouin zone increases as $\sim N^3$, see Refs. [76, 77]. The dependence of Q_{ord} on N calculated numerically for the structure under consideration is shown in Table 1.

As a next step, we account for the contribution of the structural disorder Q_{dis} to the total quality factor Q_{tot}. We will consider a model of the uncorrelated disorder introducing a fluctuation to the position of the rod keeping all the rods parallel. To gain deeper insight into how the structural disorder affects symmetry-protected and accidental BICs, we first consider the fluctuations in the rod positions along the x and y axes independently and then account for these shifts simultaneously. In both cases, the shift of the rod is given by $\delta t = R \cdot \sigma \cdot a$. Here, a is the period of the structure, σ is a fluctuation amplitude (disorder amplitude); R is a uniformly distributed random number in the range $[-1; 1]$.

To analyze Q_{dis} we use the finite element method calculating the complex eigenfrequencies and total Q factors of the disordered array of rods with the finite number of periods N. We collect the data from ensembles of 100 structures for each value of amplitude σ at the given number of periods N. Then we average the calculated Q factors over the ensemble as $\langle Q_{\text{tot}}\rangle = \sum_{i=1}^{m} Q_{\text{tot}}^i/m$, where m is the number of ensembles.

Figure 2 exhibits decreasing of the Q factor for both symmetry-protected and accidental BICs (sp-BIC and s-BIC) with the growing amplitude of disorder σ. As it was mentioned above, the in-Γ accidental BICs (a-BIC and s-BIC) require particular values of the distance between layers h at which the round-trip phase shift accumulates to a value being multiple of 2π. Therefore, the accidental BICs are more sensitive to the fluctuations in rod position along the y axis rather than along the x axis [see Figure 2(a)]. Thus, when we account the shift of rods along both coordinates, we observe that the random shifts along the y-axis make the main contribution to the decreasing of the

Table 1: Radiative Q factor (Q_{ord}) for different types of BICs in structures of finite size consisting of N periods.

Number of periods, N	100	150	200
sp-BIC	7600	22,500	47,300
a-BIC	10,300	33,900	78,800
s-BIC	7800	24,700	60,200

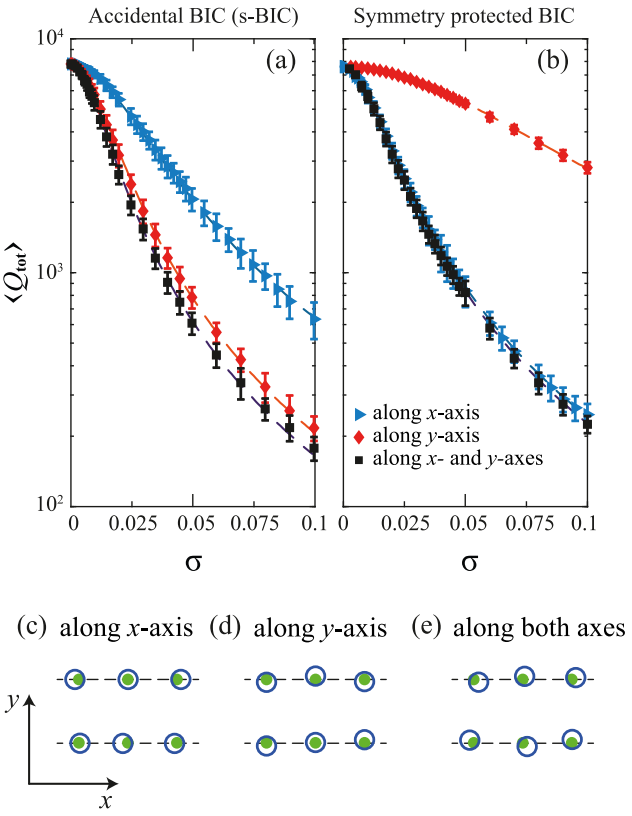

Figure 2: Dependence of average Q_{tot} of disordered structures on disorder amplitude σ for (a) the accidental s-BIC and (b) the symmetry-protected sp-BIC. Bars indicate the standard deviation. Number of periods $N = 100$. Schematic view of the rod array with the structural disorder (c) along x-axis, (d) along y-axis and (e) along both axes. Green solid circles show the ordered structure, blue open circles show the structures with disorder.

Q factor for the accidental BICs. In contrast, the symmetry-protected BIC (sp-BIC) exist at any distance between the layers (Figure 1). Therefore, the y-axis disorder does not affect much its Q factor. However, the random shifts of rods along the x-axis induce an additional polarization (dipole moment) along the x-axis resulting in radiative losses. Thus, the symmetry-protected BIC is most sensitive to the lateral shifts of meta-atoms inside the unit cell [Figure 2(b)].

Next, we calculate the dependence of the total Q factor (Q_{tot}) of the accidental s-BIC on the disorder amplitude σ for three structures of different length ($N = 100, 150, 200$) accounting for random shifts of the rods only along the x-axis [Figure 3(a)]. One can see from this figure that the Q factor becomes sensitive to structural disorder only when the disorder amplitude reaches a threshold $\sigma \sim 0.01$. For smaller σ, the Q factor is completely defined by the radiation losses due to the finite size of the structure. In contrast, for $\sigma > 0.01$ the main contribution to the radiation losses is made by the scattering events on the structural disorder resulting in quadratic decaying of the Q factor with σ. This quadratic dependence is observed for both types of the structural disorder (along the x and y axes) (see Figure 7 in Appendix A.1). The similar dependence of the Q_{dis} factor was shown recently for eigenmodes of the periodic dielectric grating composed of supercells with fluctuations in grooves positions and filling factor [56].

Next, we examine whether the losses due to disorder along the x and y axes can be decomposed into two independent terms corresponding to the disorder along each axis separately

$$\frac{1}{Q^{x,y}_{dis}} = \frac{1}{Q^{x}_{dis}} + \frac{1}{Q^{y}_{dis}}. \tag{3}$$

Usually, it is true only when the radiative losses caused due to both of these shifts are small. For a large amplitude of the disorder, the total losses might not be expanded into a sum of simple terms from each disorder obtained independently. We expect that some correlation between shifts along x and y appearing since the shape of a sole rod is conserved may impact on $Q^{x,y}_{dis}$. To analyze the validity of this decomposition, we consider an auxiliary quantity

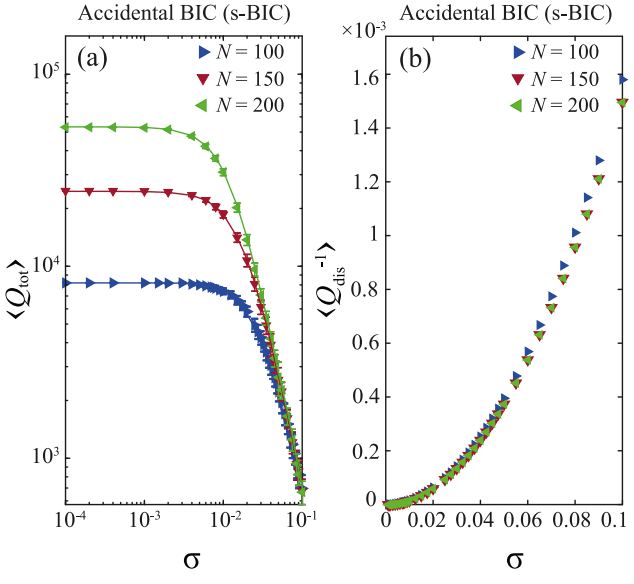

Figure 3: (a) Average Q_{tot} of the accidental s-BIC supported by the structure with disorder along x axis with different number of periods N. Vertical bars denote the standard deviation. Solid lines show the approximation. (b) Average Q^{-1}_{dis} of the accidental s-BIC supported by the structure with disorder along x axis with different number of periods N. Blue, red, and green symbols correspond to $N = 100, 150, 200$, respectively.

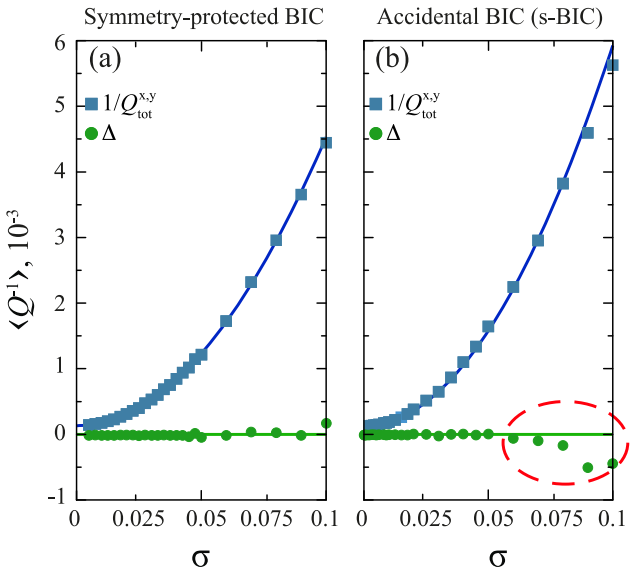

Figure 4: Average Q^{-1} of (a) the symmetry-protected BIC, (b) the accidental s-BIC. Blue squares show dependence of inverse average Q factor on the disorder degree along both axes, green points are the difference according to Eq. (4). Solid lines are guides for an eye only. Red dashed circle shows the region of σ, where Eq. (4) is not valid.

characterizing the deviation from it

$$\Delta = \frac{1}{Q^{x,y}_{\text{dis}}} - \frac{1}{Q^{x}_{\text{dis}}} - \frac{1}{Q^{y}_{\text{dis}}}. \tag{4}$$

If the composition (3) is correct then Δ has to be zero. Figure 4 demonstrates the dependence of $1/Q^{x,y}_{\text{dis}}$ and Δ on an amplitude of disorder σ for the symmetry-protected (panel a) and accidental s-BIC (panel b). As it can be seen from the figure, decomposition (3) breaks for the accidental s-BIC for $\sigma > 0.7$. This can be caused by correlation between shifts for a sole rod which impact becomes comparable with separate contributions with σ increasing. In addition to correlation, large disorder amplitudes can result in the spatial localization of the mode at a scale less than the length of the structure, thus, reducing its effective length. For the symmetry-protected BIC, there are some deviations of Δ for large σ but they are substantially smaller than ones for the accidental s-BIC. We suppose that a symmetry of field distribution plays a crucial role causing stability of sp-BICs rather than accidental BICs.

2.3 Effect of spatial localization

As we discussed previously, the Q factor of all types of BICs depends on the size of the sample. From other hand it is known that disorder can result in spatial localization of wavefunctions (eigenmodes) that can be considered as effective reduction of the sample size [50, 78–81]. In this section, we analyze how the structural disorder results in spatial localization of BICs and how it affects their Q factors.

As we discussed in the previous section, there is a deviation from Eq. (3) for large disorder amplitudes for the accidental BIC (s-BIC). We suppose that this deviation can be related to the wave localization inherited to one-dimension systems with structural disorder [50, 78], which leads to an effective reduction of the structure length. We examine the amplitude of the electric field distribution along the structures of different length.

Figure 5 shows the envelop curves (mode profiles) of the accidental BIC (s-BIC) for the structure of various length ($N = 100, 150, 200$) for the fixed disorder amplitude $\sigma = 0.085$. The shaded areas of different colors correspond to different realization from the ensemble. The gray curves correspond to the envelope function of the accidental s-BIC in structures without disorder. To estimate the localization length, we superpose the envelope function of the accidental s-BIC in structure with $N = 60$ (dashed curve). One can see that for disorder amplitude $\sigma = 0.085$ the wavefunction is localized on around 60 periods for all x-, y- or xy-oriented disorder. From one hand, the structural disorder localizes the wavefunction inside the structure, thus, the losses due radiation from the ends of the chain are negligible. Therefore, this loss mechanism is essential as for regular structure. From other hand, the structural disorder reduces the effective length of the structure limiting the Q factor. The localization can be neglected for the most practical shorter structures; it has to be taken into account for larger, self-assembled, and natural structures, though.

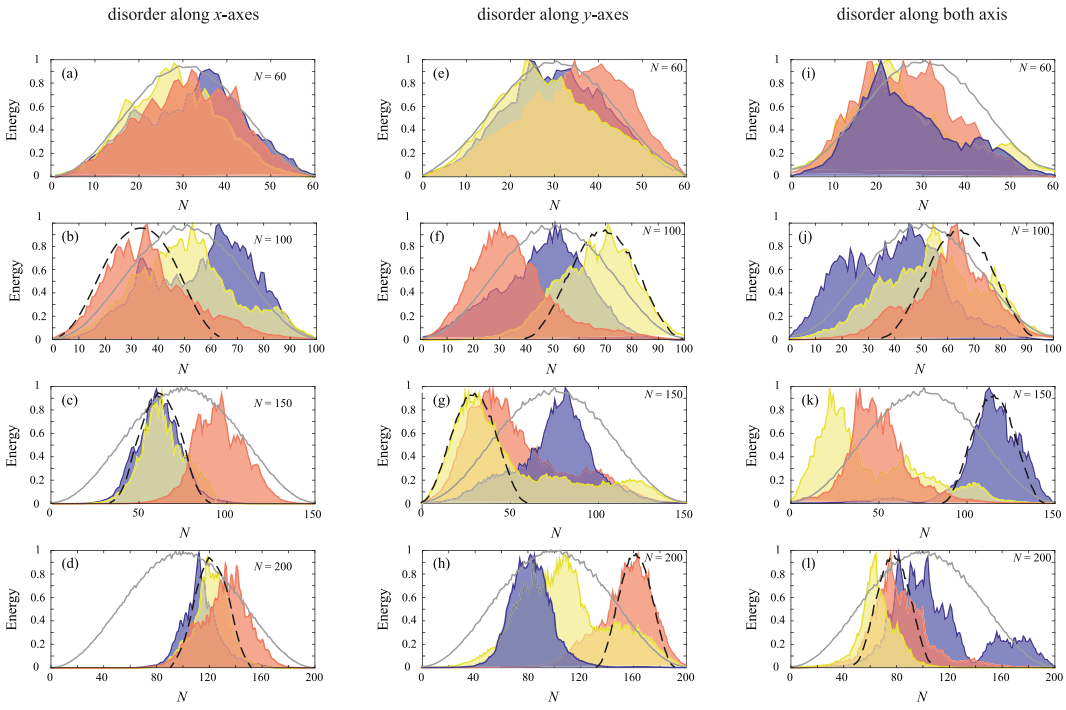

Figure 5: Electromagnetic energy distribution along chain at the accidental BIC (s-BIC). Curves with shaded area with different colors show several realization of the disorder $\sigma = 0.085$. Gray curves are the distribution for the structures with no disorder. (a, e, i) $N = 60$, (b, f, j) $N = 100$, (c, g, k) $N = 150$, (d, h, l) $N = 200$. The black dashed curves show the energy distribution in the chain of $N = 60$ with no disorder $\sigma = 0$ for comparison.

3 Conclusions

In conclusion, we have uncovered how the uncorrelated structural disorder affects the symmetry-protected and accidental in-Γ BICs in the one-dimensional periodic structure composed of two layers of dielectric rods. Regardless of the direction along which the position of rods are perturbed, the Q factor of both symmetry-protected and accidental BICs decays quadratically with the amplitude of the disorder σ. Importantly, the symmetry-protected BIC is more resistant to the fluctuation of the distance between layers (along y) rather than the fluctuation of position along x. And vice versa, the accidental BIC is more robust against the fluctuation along the direction of periodicity (along x). We have shown that the fluctuations of position along the direction of periodicity and distance between the layers contribute to the losses independently for low disorder amplitudes. For the large values of disorder amplitude σ or long structures, the localization of electromagnetic energy suppresses the total Q factor due to the effective reduction of the system length. We anticipate our findings provide useful guidelines for practical implementation of resonators supporting bound states in the continuum in self-assembled and natural structures, where the role of structural disorder is the most relevant.

Author contribution: All the authors have accepted responsibility for the entire content of this submitted manuscript and approved submission.

Research funding: Simulations of eigenmodes of disordered structures were supported by the Russian Science Foundation (20-72-00152). Analysis of disorder strength on BIC and their robustness and effect of spatial localization was supported by Russian Science Foundation (21-19-00677). A.B. acknowledges the BASIS foundation and the Council on Grants of the President of the Russian Federation (MK-2224.2020.2).

Conflict of interest statement: The authors declare no conflicts of interest regarding this article.

Appendix A: BIC's frequency in a periodic structure without disorder

Figure 6 shows how the frequencies of sp-, a-, and s-BICs depend on the distance between layers h of the infinite periodic structure. While the frequency of the sp-BIC

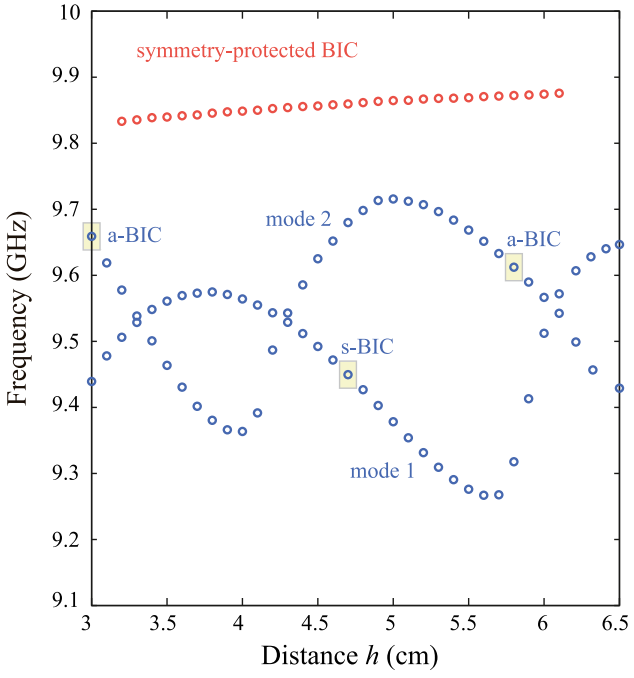

Figure 6: Frequency of three lowest modes of the structure under consideration. The symmetry-protected BIC is denoted as sp-BIC, symmetric accidental BIC – as s-BIC, asymmetric accidental BIC – as a-BIC. The yellow rectangles correspond to accidental BICs [see Figure 1(b)].

increases slowly, the frequencies of the mode 1 and mode 2, at which the accidental BICs occur, exhibit complicate behavior.

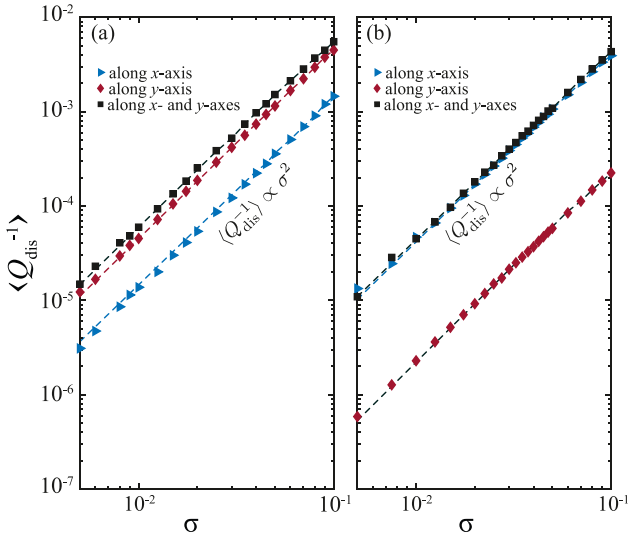

Figure 7: Average Q_{dis}^{-1} factor of (a) the accidental BIC and (b) symmetry-protected BIC supported by the structure with disorder. Dashed lines show quadratic approximation.

A.1 Radiative losses due to structural disorder

Figure 7 shows that, for both symmetry-protected and accidental BICs, the losses due to various types of structural disorder exhibit quadratic dependence on the disorder amplitude.

References

[1] J. von Neumann and E. P. Wigner, "Über merkwürdige diskrete eigenwerte," *Z. Phys.*, vol. 30, p. 465, 1929.
[2] C. W. Hsu, B. Zhen, A. D. Stone, J. D. Joannopoulos, and M. Soljačić, "Bound states in the continuum," *Nat. Rev. Mater.*, vol. 1, p. 16048, 2016.
[3] K. Koshelev, A. Bogdanov, and Y. Kivshar, "Meta-optics and bound states in the continuum," *Sci. Bull.*, vol. 64, pp. 836–842, 2018.
[4] S. Han, L. Cong, Y. K. Srivastava, et al., "All-dielectric active terahertz photonics driven by bound states in the continuum," *Adv. Mater.*, vol. 31, p. 1901921, 2019.
[5] E. N. Bulgakov and A. F. Sadreev, "Bound states in the continuum with high orbital angular momentum in a dielectric rod with periodically modulated permittivity," *Phys. Rev. A*, vol. 96, p. 013841, 2017.
[6] E. N. Bulgakov and A. F. Sadreev, "Light trapping above the light cone in a one-dimensional array of dielectric spheres," *Phys. Rev. A*, vol. 92, p. 023816, 2015.
[7] Z. Sadrieva, M. Belyakov, M. Balezin, et al., "Experimental observation of a symmetry-protected bound state in the continuum in a chain of dielectric disks," *Phys. Rev. A*, vol. 99, p. 053804, 2019.
[8] M. Sidorenko, O. Sergaeva, Z. Sadrieva, et al., "Observation of an accidental bound state in the continuum in a chain of dielectric disks," *Phys. Rev. Appl.*, vol. 15, p. 034041, 2021.
[9] C.-L. Zou, J.-M. Cui, F.-W. Sun, et al., "Guiding light through optical bound states in the continuum for ultrahigh-q microresonators," *Laser Photon. Rev.*, vol. 9, p. 114, 2015.
[10] Z. Yu, X. Xi, J. Ma, H. K. Tsang, C.-L. Zou, and X. Sun, "Photonic integrated circuits with bound states in the continuum," *Optica*, vol. 6, p. 1342, 2019.
[11] E. N. Bulgakov and A. F. Sadreev, "Bound states in the continuum in photonic waveguides inspired by defects," *Phys. Rev. B*, vol. 78, p. 075105, 2008.
[12] E. A. Bezus, D. A. Bykov, and L. L. Doskolovich, "Bound states in the continuum and high-q resonances supported by a dielectric ridge on a slab waveguide," *Photon. Res.*, vol. 6, p. 1084, 2018.
[13] D. A. Bykov, E. A. Bezus, and L. L. Doskolovich, "Bound states in the continuum and strong phase resonances in integrated Gires–Tournois interferometer," *Nanophotonics*, vol. 9, p. 83, 2020.
[14] M. V. Rybin, K. L. Koshelev, Z. F. Sadrieva, et al., "High-q supercavity modes in subwavelength dielectric resonators," *Phys. Rev. Lett.*, vol. 119, p. 243901, 2017.
[15] L. Carletti, K. Koshelev, C. De Angelis, and Y. Kivshar, "Giant nonlinear response at the nanoscale driven by bound states in

the continuum," *Phys. Rev. Lett.*, vol. 121, p. 033903, 2018.
[16] M. Odit, K. Koshelev, S. Gladyshev, K. Ladutenko, Y. Kivshar, and A. Bogdanov, "Observation of supercavity modes in subwavelength dielectric resonators," *Adv. Mater.*, vol. 33, p. 2003804, 2021.
[17] A. Kodigala, T. Lepetit, Q. Gu, B. Bahari, Y. Fainman, and B. Kanté, "Lasing action from photonic bound states in continuum," *Nature*, vol. 541, p. 196, 2017.
[18] B. Wang, W. Liu, M. Zhao, et al., "Generating optical vortex beams by momentum-space polarization vortices centred at bound states in the continuum," *Nat. Photonics*, vol. 14, pp. 1–6, 2020.
[19] C. Cui, C. Zhou, S. Yuan, et al., "Multiple fano resonances in symmetry-breaking silicon metasurface for manipulating light emission," *ACS Photonics*, vol. 5, p. 4074, 2018.
[20] B. Midya and V. V. Konotop, "Coherent-perfect-absorber and laser for bound states in a continuum," *Opt. Lett.*, vol. 43, p. 607, 2018.
[21] Q. Song, J. Hu, S. Dai, et al., "Coexistence of a new type of bound state in the continuum and a lasing threshold mode induced by pt symmetry," *Sci. Adv.*, vol. 6, p. eabc1160, 2020.
[22] S. Mohamed, J. Wang, H. Rekola, et al., Topological charge engineering in lasing bound states in continuum, 2020, arXiv preprint arXiv:2012.15642.
[23] M.-S. Hwang, H.-C. Lee, K.-H. Kim, et al., "Ultralow-threshold laser using super-bound states in the continuum," *Nat. Commun.*, vol. 12, p. 1, 2021.
[24] M. Wu, S. T. Ha, S. Shendre, et al., "Room-temperature lasing in colloidal nanoplatelets via mie-resonant bound states in the continuum," *Nano Lett.*, vol. 20, p. 6005, 2020.
[25] S. T. Ha, Y. H. Fu, N. K. Emani, et al., "Directional lasing in resonant semiconductor nanoantenna arrays," *Nat. Nanotechnol.*, vol. 13, p. 1042, 2018.
[26] J. M. Foley, S. M. Young, and J. D. Phillips, "Symmetry-protected mode coupling near normal incidence for narrow-band transmission filtering in a dielectric grating," *Phys. Rev. B*, vol. 89, p. 165111, 2014.
[27] J. M. Foley and J. D. Phillips, "Normal incidence narrowband transmission filtering capabilities using symmetry-protected modes of a subwavelength, dielectric grating," *Opt. Lett.*, vol. 40, p. 2637, 2015.
[28] X. Cui, H. Tian, Y. Du, G. Shi, and Z. Zhou, "Normal incidence filters using symmetry-protected modes in dielectric subwavelength gratings," *Sci. Rep.*, vol. 6, p. 36066, 2016.
[29] S. Romano, G. Zito, S. Managò, et al., "Surface-enhanced Raman and fluorescence spectroscopy with an all-dielectric metasurface," *J. Phys. Chem. C*, vol. 122, p. 19738, 2018.
[30] S. Romano, G. Zito, S. Torino, et al., "Label-free sensing of ultralow-weight molecules with all-dielectric metasurfaces supporting bound states in the continuum," *Photon. Res.*, vol. 6, p. 726, 2018.
[31] Y. K. Srivastava, R. T. Ako, M. Gupta, M. Bhaskaran, S. Sriram, and R. Singh, "Terahertz sensing of 7 nm dielectric film with bound states in the continuum metasurfaces," *Appl. Phys. Lett.*, vol. 115, p. 151105, 2019.
[32] X. Chen, W. Fan, and H. Yan, "Toroidal dipole bound states in the continuum metasurfaces for terahertz nanofilm sensing," *Opt. Express*, vol. 28, p. 17102, 2020.
[33] D. N. Maksimov, V. S. Gerasimov, S. Romano, and S. P. Polyutov, "Refractive index sensing with optical bound states in the continuum," *Opt. Express*, vol. 28, p. 38907, 2020.
[34] Y. Kivshar and A. Miroshnichenko, "Meta-optics with mie resonances," *Opt. Photon. News*, vol. 28, p. 24, 2017.
[35] K. Koshelev, Y. Tang, K. Li, D.-Y. Choi, G. Li, and Y. Kivshar, "Nonlinear metasurfaces governed by bound states in the continuum," *ACS Photonics*, vol. 6, p. 1639, 2019.
[36] S. Krasikov, A. Bogdanov, and I. Iorsh, "Nonlinear bound states in the continuum of a one-dimensional photonic crystal slab," *Phys. Rev. B*, vol. 97, p. 224309, 2018.
[37] L. Carletti, K. Koshelev, C. De Angelis, and Y. Kivshar, "Giant nonlinear response at the nanoscale driven by bound states in the continuum," *Phys. Rev. Lett.*, vol. 121, p. 033903, 2018.
[38] E. N. Bulgakov and D. N. Maksimov, "Nonlinear response from optical bound states in the continuum," *Sci. Rep.*, vol. 9, p. 1, 2019.
[39] V. Kravtsov, E. Khestanova, F. A. Benimetskiy, et al., "Nonlinear polaritons in a monolayer semiconductor coupled to optical bound states in the continuum," *Light Sci. Appl.*, vol. 9, p. 1, 2020.
[40] L. Carletti, S. S. Kruk, A. A. Bogdanov, C. De Angelis, and Y. Kivshar, "High-harmonic generation at the nanoscale boosted by bound states in the continuum," *Phys. Rev. Res.*, vol. 1, p. 023016, 2019.
[41] A. P. Anthur, H. Zhang, R. Paniagua-Dominguez, et al., "Continuous wave second harmonic generation enabled by quasi-bound-states in the continuum on gallium phosphide metasurfaces," *Nano Lett.*, vol. 20, p. 8745, 2020.
[42] D. N. Maksimov, A. A. Bogdanov, and E. N. Bulgakov, "Optical bistability with bound states in the continuum in dielectric gratings," *Phys. Rev. A*, vol. 102, p. 033511, 2020.
[43] K. Koshelev, S. Kruk, E. Melik-Gaykazyan, et al., "Subwavelength dielectric resonators for nonlinear nanophotonics," *Science*, vol. 367, p. 288, 2020.
[44] I. V. Timofeev, D. N. Maksimov, and A. F. Sadreev, "Optical defect mode with tunable q factor in a one-dimensional anisotropic photonic crystal," *Phys. Rev. B*, vol. 97, p. 024306, 2018.
[45] A. Taghizadeh and I.-S. Chung, "Quasi bound states in the continuum with few unit cells of photonic crystal slab," *Appl. Phys. Lett.*, vol. 111, p. 031114, 2017.
[46] Z. F. Sadrieva, I. S. Sinev, K. L. Koshelev, et al., "Transition from optical bound states in the continuum to leaky resonances: role of substrate and roughness," *ACS Photonics*, vol. 4, p. 723, 2017.
[47] K. Koshelev, S. Lepeshov, M. Liu, A. Bogdanov, and Y. Kivshar, "Asymmetric metasurfaces with high-q resonances governed by bound states in the continuum," *Phys. Rev. Lett.*, vol. 121, p. 193903, 2018.
[48] P.-E. Wolf and G. Maret, "Weak localization and coherent backscattering of photons in disordered media," *Phys. Rev. Lett.*, vol. 55, p. 2696, 1985.

[49] D. S. Wiersma, P. Bartolini, A. Lagendijk, and R. Righini, "Localization of light in a disordered medium," *Nature*, vol. 390, p. 671, 1997.
[50] A. N. Poddubny, M. V. Rybin, M. F. Limonov, and Y. S. Kivshar, "Fano interference governs wave transport in disordered systems," *Nat. Commun.*, vol. 3, p. 1, 2012.
[51] M. F. Limonov and M. Richard, *Optical Properties of Photonic Structures: Interplay of Order and Disorder*, Boca Raton, CRC Press, 2012.
[52] C. Liu, M. V. Rybin, P. Mao, S. Zhang, and Y. Kivshar, "Disorder-immune photonics based on mie-resonant dielectric metamaterials," *Phys. Rev. Lett.*, vol. 123, p. 163901, 2019.
[53] J. F. Galisteo-López, M. Ibisate, R. Sapienza, L. S. Froufe-Pérez, Á. Blanco, and C. López, "Self-assembled photonic structures," *Adv. Mater.*, vol. 23, p. 30, 2011.
[54] V. Astratov, A. Adawi, S. Fricker, M. Skolnick, D. Whittaker, and P. Pusey, "Interplay of order and disorder in the optical properties of opal photonic crystals," *Phys. Rev. B*, vol. 66, p. 165215, 2002.
[55] S. Fan, P. R. Villeneuve, and J. Joannopoulos, "Theoretical investigation of fabrication-related disorder on the properties of photonic crystals," *J. Appl. Phys.*, vol. 78, p. 1415, 1995.
[56] L. Ni, J. Jin, C. Peng, and Z. Li, "Analytical and statistical investigation on structural fluctuations induced radiation in photonic crystal slabs," *Opt. Express*, vol. 25, p. 5580, 2017.
[57] Y.-X. Xiao, Z.-Q. Zhang, and C. Chan, "A band of bound states in the continuum induced by disorder," *Sci. Rep.*, vol. 8, p. 1, 2018.
[58] H. L. Chen, G. Wang, and R. K. Lee, "Nearly complete survival of an entangled biphoton through bound states in continuum in disordered photonic lattices," *Opt. Express*, vol. 26, p. 33205, 2018.
[59] Y.-S. Jin, G.-J. Kim, and S.-G. Jeon, "Terahertz dielectric properties of polymers," *J. Kor. Phys. Soc.*, vol. 49, p. 513, 2006.
[60] R. Haas and P. Zimmermann, "22-Ghz measurements of dielectric constants and loss tangents of castable dielectrics at room and cryogenic temperatures," *IEEE T. Microw. Theory*, vol. 24, p. 881, 1976.
[61] R. F. Ndangali and S. V. Shabanov, "Electromagnetic bound states in the radiation continuum for periodic double arrays of subwavelength dielectric cylinders," *J. Math. Phys.*, vol. 51, p. 102901, 2010.
[62] F. R. Ndangali and S. V. Shabanov, "The resonant nonlinear scattering theory with bound states in the radiation continuum and the second harmonic generation," in *Active Photonic Materials V*, vol. 8808, San Diego, International Society for Optics and Photonics, 2013, p. 88081F.
[63] E. Bulgakov, D. Maksimov, P. Semina, and S. Skorobogatov, "Propagating bound states in the continuum in dielectric gratings," *J. Opt. Soc. Am. B*, vol. 35, p. 1218, 2018.
[64] H. Hemmati and R. Magnusson, "Resonant dual-grating metamembranes supporting spectrally narrow bound states in the continuum," *Adv. Opt. Mater.*, vol. 7, p. 1900754, 2019.
[65] Y. Shuai, D. Zhao, Z. Tian, et al., "Double-layer Fano resonance photonic crystal filters," *Opt. Express*, vol. 21, p. 24582, 2013.
[66] Y. Shuai, D. Zhao, A. S. Chadha, et al., "Coupled double-layer Fano resonance photonic crystal filters with lattice-displacement," *Appl. Phys. Lett.*, vol. 103, p. 241106, 2013.
[67] D. Marinica, A. Borisov, and S. Shabanov, "Bound states in the continuum in photonics," *Phys. Rev. Lett.*, vol. 100, p. 183902, 2008.
[68] C. W. Hsu, B. Zhen, J. Lee, et al., "Observation of trapped light within the radiation continuum," *Nature*, vol. 499, p. 188, 2013.
[69] B. Zhen, C. W. Hsu, L. Lu, A. D. Stone, and M. Soljačić, "Topological nature of optical bound states in the continuum," *Phys. Rev. Lett.*, vol. 113, p. 257401, 2014.
[70] E. N. Bulgakov and D. N. Maksimov, "Topological bound states in the continuum in arrays of dielectric spheres," *Phys. Rev. Lett.*, vol. 118, p. 267401, 2017.
[71] K. Sakoda, *Optical Properties of Photonic Crystals*, Berlin, Springer, 2005.
[72] E. Ivchenko and G. Pikus, "Crystal symmetry," in *Superlattices and Other Heterostructures*, *Springer Series in Solid-State Sciences*, vol. 110, Berlin, Heidelberg, Springer, 1995.
[73] V. Karagodsky, C. Chase, and C. J. Chang-Hasnain, "Matrix fabry–perot resonance mechanism in high-contrast gratings," *Opt. Lett.*, vol. 36, p. 1704, 2011.
[74] V. Karagodsky and C. J. Chang-Hasnain, "Physics of near-wavelength high contrast gratings," *Opt. Express*, vol. 20, p. 10888, 2012.
[75] Z. F. Sadrieva, M. A. Belyakov, M. A. Balezin, et al., "Experimental observation of a symmetry-protected bound state in the continuum in a chain of dielectric disks," *Phys. Rev. A*, vol. 99, p. 053804, 2019.
[76] E. N. Bulgakov and D. N. Maksimov, "Light enhancement by quasi-bound states in the continuum in dielectric arrays," *Opt. Express*, vol. 25, p. 14134, 2017.
[77] E. N. Bulgakov and A. F. Sadreev, "High-q resonant modes in a finite array of dielectric particles," *Phys. Rev. A*, vol. 99, p. 033851, 2019.
[78] I. Lifshits, S. Gredeskul, and L. Pastur, *Introduction to the Theory of Disordered Systems*, New York, Wiley, 1988.
[79] F. Evers and A. D. Mirlin, "Anderson transitions," *Rev. Mod. Phys.*, vol. 80, p. 1355, 2008.
[80] J. Billy, V. Josse, Z. Zuo, et al., "Direct observation of anderson localization of matter waves in a controlled disorder," *Nature*, vol. 453, p. 891, 2008.
[81] M. Segev, Y. Silberberg, and D. N. Christodoulides, "Anderson localization of light," *Nat. Photonics*, vol. 7, p. 197, 2013.